RESISTANCE STRAIN GAGES FILLAMENTS EFFECT

Nashwan T. Younis, *Younis@engr.ipfw.edu* Department of Mechanical Engineering, Indiana University-Purdue University Fort Wayne, USA

Bongsu Kang, *kang@engr.ipfw.edu* Department of Mechanical Engineering, Indiana University-Purdue University Fort Wayne, USA

ABSTRACT

The subject of error using strain gages is complex and it is not the intension to present a comprehensive analysis. In this study, the discrete averaging effects of a strain gage along the gage filaments are taken into account in the assessment of the errors due to placement of the gage, gage length, gage width, and number of filaments. The gage is placed near the edge of a hole in an infinite plate subjected uniaxial tension. It is shown that the average strain over the gage filaments is not the same as the average strain over the gage grid area. Recommendations for selecting gages are presented.

Keywords: Experimental stress analysis, Strain gage

INTRODUCTION

Most people come across strain gage based devices on a daily basis but unaware of the fact. Experimental stress analysis engineers have both personal and professional interaction with strain gages and perhaps are no more aware of the background about the magnitude of averaging effects of gages or the principle of strain gages. In 2006, Robinson discussed the fact that stress analysis engineers probably no more aware of the background regarding some aspects of the gages than the average person [1]. Solving tough strain gage problems becoming what was old and unsolved is new again. Cappa et al. [2] developed a conditioning unit based on the direct resistance measurement method by driving a constant current through a strain gage. Ajovalasit's [3] analysis showed the output of a strain gage is influenced by the coupled effect of transverse sensitivity and pressure sensitivity on the gage. An experimental method was developed to determine the stiffness of some commercial strain gages [4]. The results showed that strain gage stiffness is a feature to be considered for the evaluation of the local and global reinforcement effects.

Strain gages are accurate when the gage is placed on isotropic materials with relatively uniform stress distributions. However, the accuracy of the strain gage is not always high. Error is introduced from the physical nature of the strain gage and how it measures the strain. The error is acceptable, but increases significantly when the gage is used to measure strain at discontinuities such as holes, notches, and crack tip; areas of steep strain gradients. In the field of fracture mechanics, some researchers use the gage reading as the strain at the center of the gage. This is not an accurate representation of the stress field at a crack tip due to the averaging effect. Irwin suggested that mode

one stress-intensity factor, K_I, near a crack tip can be determined experimentally by using strain gages [5]. In 1987 Dally and Sanford developed a method that utilizes strain gages for determining K_I [6]. An overdeterministic approach was developed for measuring K_I using data from three 10-element strip strain gages with some accuracy [7]. The error generated in K_I due to placement errors in positioning and orienting the single gage was determined [8]. It was concluded that the deviation in the orientation angle of the strain gage is the dominant source of the error. A technique for stress intensity factor determination using strain gages was developed in which the location of the strain gage relative to the crack tip was chosen through parametric study of the asymptotic fields [9]. Sarangi et al. [10] proposed a finite element based method for determining the limiting radial distance of placing the strain gage in the vicinity of a crack tip.

Recently, the effect of strain gradient was mentioned or ignored by researchers in the field. To assure accuracy of determining structural gage sensitivity, Zhang et al. chose locations for the strain gage rosettes with small strain gradient [11]. Hole-drilling method is the most common technique for measuring residual stresses in various materials and structures [12]. It utilizes strain gages around circular hole. The averaging effect of the gage around the hole is ignored, perhaps due to the difficulty in estimating the magnitude of the error. The correction of errors introduced by hole eccentricity has been proposed by Barsanescu and Carlescu [13]. In 2009, the performance of three dimensional strain gages embedded into a sphere was evaluated [14]. In the case of high strain gradient, the calculated strain tensor is subject to errors and this problem can be overcome by embedding the gages in a sphere at a specified orientation relative to the center of the sphere.

The subject of error in a strain measurement system using metal-foil sensing grid is complex. In 1984, Pople listed the human factor errors and error sources in strain gage measurement [15]. Perry presented an extensive report that examined several fundamental properties of the strain gage that are involved in measurement accuracy [16]. These properties are the gage factor, reinforcement effects, transverse sensitivity, and thermal effects. In addition, Perry plotted the percentage difference between the peak strain at a hole and the strain integrated over the gage square area against the ratio of the grid area to hole radius. The traditional method of examining the strain averaging is to use the average strain over the area of the entire strain gage grid. The gage filament covers only a portion of this area, and this fact needs to be accounted for in an analysis of errors due to strain gage placement. The average strain over the gage filaments is not the same as the average strain over the gage grid area. In a series of articles deal with resistance strain gages, Stein shared his experience that he developed over more than forty years [17]. The articles are about transducers and signal conditioning as strain gages are made of resistive filaments.

Strain gages are available in many different sizes and configurations. Therefore, understanding the

variables in the averaging effect will result in proper gage selection. In this paper, a comprehensive analysis of the discrete averaging effect associated with high strain gradient is presented. Recommendations are made for selecting gages for high strain gradient measurements at the end. The strain averaging is modeled with the intention of extracting sufficient knowledge to illustrate the typical results that can be expected from strain gages at stress concentration areas. A classical plate with a circular hole subjected to uniaxial loading is used as a vehicle for examining the effects of gage length, gage width, number of filaments, and gage misplacement on the average strain experienced by the gage.

THEORY

The strain gage is a type of electrical resistor. Most commonly, strain gages are thin metal-foil grids that are bonded to the surface of a machine part or a structural member. When forces are applied to the member, the gage elongates or contracts with the member, creating normal strains. The change in length of the gage alters its electrical resistance. By measuring the electrical resistance of the wire, the gage can be calibrated to read values of normal strain directly.

Since the gage is of finite length, the change in resistance is due to the average strain along the gage and not the center strain in general. If the strain along the gage is constant or linear, the average strain is the same as that of the center strain. However, for a stress concentration problem, the average strain will differ from the center strain. When the strain gradient is large, the average strain is lower than the true strain at a point. Therefore, the indicated strain will be in error of the true strain.

The photoetching process used to create the metal-foil grids is very versatile, enabling a wide verity of gage sizes and grid shapes to be produced [18]. The grid is bonded to a thin plastic backing film or carrier because the foil is fragile. The backing provides three main functions:

1. Means of handling the foil during the installation process of the strain gage
2. Bondable surface for adhering the gage to the specimen
3. Electrical insulation between the gage and the object being tested
4. Space for alignment markings and solder tabs to attach the lead wires

It is clear that the thin plastic backing is an integral part to the basic gage construction. However, conformance to measure peak strain in the vicinity of stress concentration will be reduced.

Each gage consists of a fine metal grid that is stretched or shortened when the object is strained at the area where the gage is attached. The grid is equivalent to a continuous wire that goes back and forth from one end of the grid to the other, therefore effectively increasing its length. The grid of bonded foil gage, shown in Fig. 1, is the major source of error introduced by the strain gage when it is used to measure strain at the edge of the hole. The electrical resistance strain gage measures the average strain of each filament and the indicated strain is the average of the filaments strains. Using the points shown in Fig. 1, the indicated strain is:

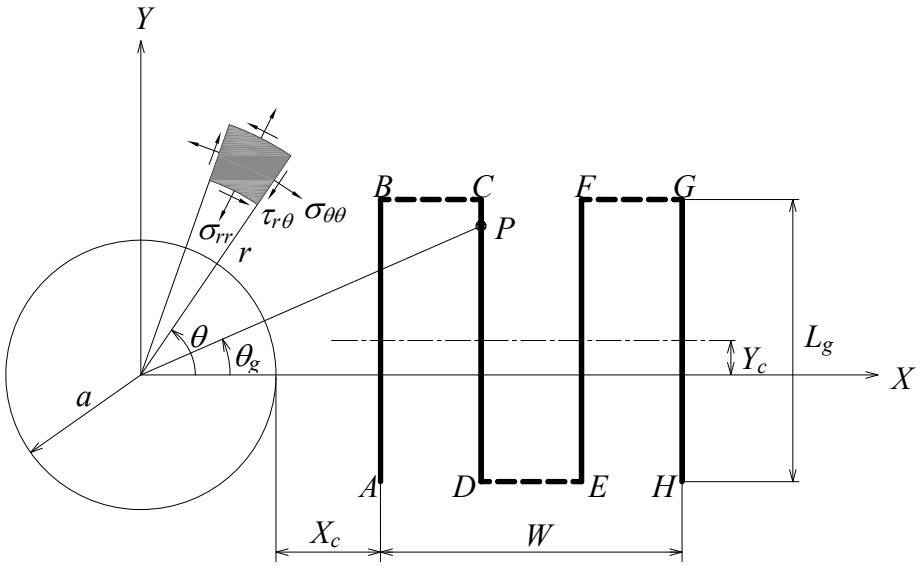

Figure 1. Definition of the Strain Gage Geometry.

$$\varepsilon_{\text{indicated}} = \frac{\varepsilon_{AB} + \varepsilon_{CD} + \varepsilon_{EF} + \varepsilon_{GH}}{\text{number of filaments}} \tag{1}$$

One of the most important problems in the design of plate structures is to determine the stress concentration due to the presence of holes and other discontinuities. The classical Kirsch [19] solution for the stresses around a circular hole in a large plate with normal stress σ_0 applied at infinity in the *Y*-direction, as shown in Fig. 1, is given by:

$$\sigma_{rr} = \frac{\sigma_0}{2}\left[\left(1-\frac{a^2}{r^2}\right)\left(1+\left(3\frac{a^2}{r^2}-1\right)\cos 2\theta\right)\right] \tag{2.1}$$

$$\sigma_{\theta\theta} = \frac{\sigma_0}{2}\left[\left(1+\frac{a^2}{r^2}\right)+\left(1+3\frac{a^4}{r^4}\right)\cos 2\theta\right] \tag{2.2}$$

$$\tau_{r\theta} = \frac{\sigma_0}{2}\left[\left(1+3\frac{a^2}{r^2}\right)\left(1-\frac{a^2}{r^2}\right)\sin 2\theta\right] \tag{2.3}$$

In the end, the strain averaging of the gage is computed by integrating the strains along the gage filaments, for which the strain in the *Y*-direction is needed along each filament. This requires converting the stresses in the *r*-θ coordinate system to ones in the *X*-*Y* coordinate system. Upon applying the standard stress transformation equations, the stresses at point *P* can be found by:

$$\sigma_X = \sigma_{rr}\cos^2\theta_g + \sigma_{\theta\theta}\sin^2\theta_g + 2\tau_{r\theta}\cos\theta_g\sin\theta_g \tag{3.1}$$

$$\sigma_Y = \sigma_{rr}\sin^2\theta_g + \sigma_{\theta\theta}\cos^2\theta_g + 2\tau_{r\theta}\cos\theta_g\sin\theta_g \tag{3.2}$$

or, since $r^2 = X^2 + Y^2$ and $\theta_g = \tan^{-1}(Y/X)$,

$$\sigma_x = \frac{\sigma_0}{2}\left[\frac{1}{\bar{r}^2}\left(1-\frac{3}{\bar{r}^2}\right)+\frac{6}{\bar{r}^4}\left(\frac{2}{\bar{r}^2}-1\right)x^2+\frac{4}{\bar{r}^6}\left(2-\frac{3}{\bar{r}^2}\right)x^4+\frac{4}{\bar{r}^6}\left(\frac{3}{\bar{r}^2}-2\right)x^2y^2\right] \tag{4.1}$$

$$\sigma_y = \frac{\sigma_0}{2}\left[2-\frac{1}{\bar{r}^2}\left(1-\frac{3}{\bar{r}^2}\right)+\frac{2}{\bar{r}^4}\left(1-\frac{6}{\bar{r}^2}\right)x^2-\frac{4}{\bar{r}^4}y^2+\frac{12}{\bar{r}^8}x^4+\frac{4}{\bar{r}^6}\left(4-\frac{3}{\bar{r}^2}\right)x^2y^2\right] \tag{4.2}$$

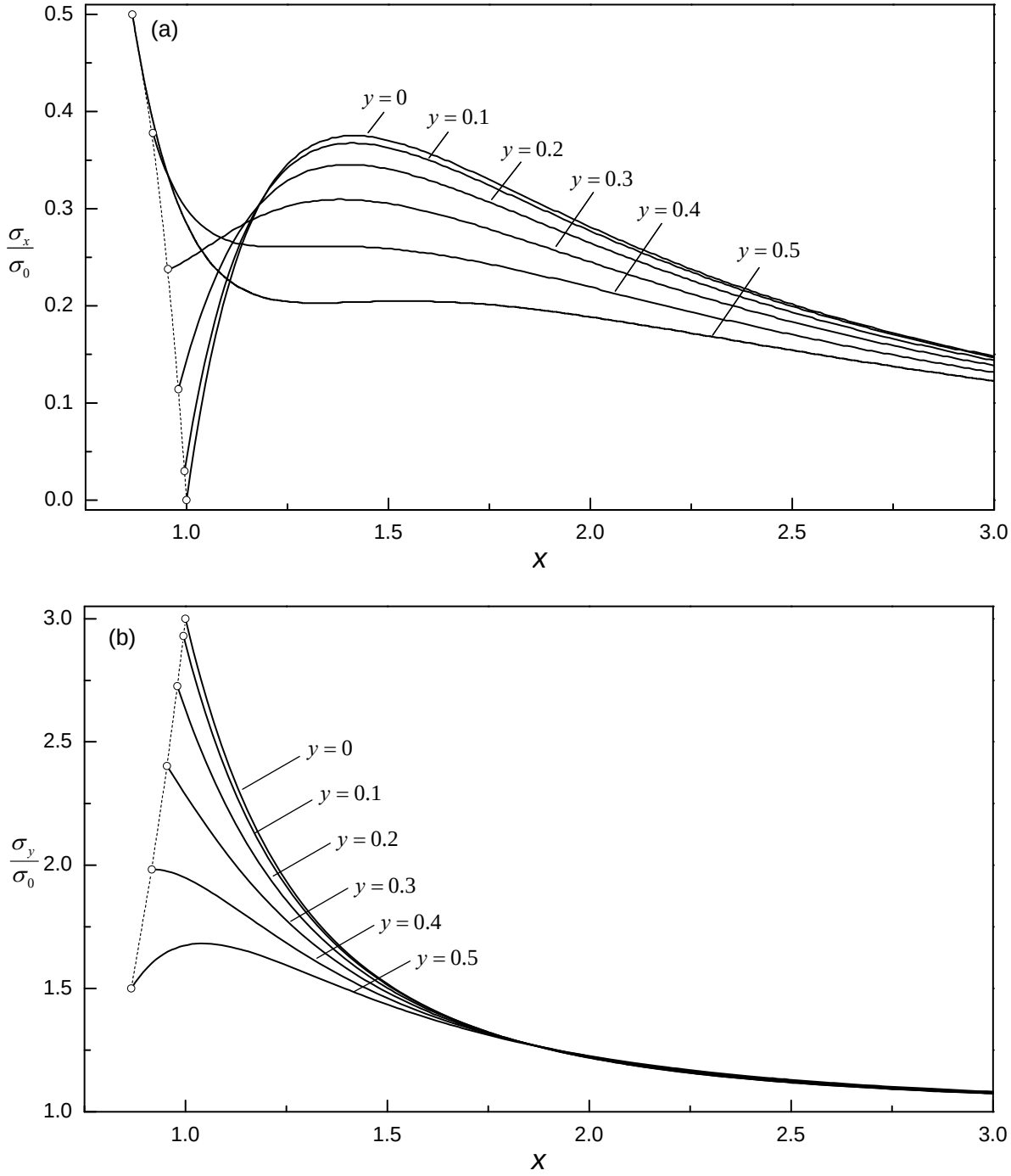

Figure 2. Distribution of (a) σ_x/σ_o and (b) σ_y/σ_o Along the x-axis Around the Hole's Boundary for ν=0.3.

Note that the X- and Y-coordinate have been normalized against the hole's radius; i.e., $x=X/a$, $y=Y/a$, and $\bar{r}^2 = x^2 + y^2$.

The distribution of σ_x/σ_o is plotted as a function of position along the x axis for various values of y in Fig. 2a. An examination of this figure clearly indicates that the transverse stress is zero at the edge of the hole (x=0) and varies in different patterns as y increases from 0 to 0.5. Thus, there is no area to mount the gage on that will represent the average σ_x. A perfect gage installation would be a x=1 when

the gage filaments are perpendicular to the x axis. To account for the expertise of the user (tilting the gage), the distributions at x less than 1 is plotted. With the hole center at the origin, the variation of σ_y/σ_o of Eq. (4.2) in the x direction at y=0, 0.1, 0.2, 0.3, 0.4, 0.5 is plotted in Fig. 2b. Examining the stress curves, one can see that the slopes change not only in magnitude, but also in sign, from negative to positive and vice versa.

Stress is a mathematical abstraction, and it can not be measured. Strains, on the other hand, can be measured directly through well-established experimental procedures such as strain gages. Once the strains in a component have been measured, the corresponding stresses can be calculated using stress-strain relationships such as generalized Hook's law. However, in this paper, the strains need to be calculated utilizing the stress equations. The stress-strain relations for a two-dimensional state of stress are:

$$\varepsilon_x = \frac{1}{E}\left(\sigma_x - \nu\sigma_y\right) \qquad \varepsilon_y = \frac{1}{E}\left(\sigma_y - \nu\sigma_x\right) \qquad (5.1\text{-}2)$$

Shown in Fig. 3 is the distribution of ε_y in the first quadrant of the x-y plane for σ_y/E=1 and ν=0.3. It can be seen that the maximum value is 3 at x=1 and y=0, which is well known as the maximum stress concentration factor σ_y/σ_o for the present case. Note also that, although not clearly shown in the graph, ε_y=ν at x=0 and y=1 since σ_x/σ_o=1 and σ_y=0 at that point. The results show that the average strain does not equal the strain at the gage center.

The traditional method of examining the strain averaging is to use the average strain over the area of the entire strain gage grid. However, the gage filament covers only a portion of this area as shown in Fig. 1. This fact needs to be accounted for in an analysis of errors due to strain gage placement. The strain averaging of the gage is modeled by integrating the strains along the filaments. Thus, the strain in the y direction is needed along each filament. The last step is to compute the average strain experienced by n filaments placed in the y-direction, which can be found by:

$$\varepsilon_{avg} = \frac{1}{nl_g}\sum_{k=1}^{n}\int_{l_g}\varepsilon_{yk}\,dy \qquad (6)$$

where $l_g=L_g/a$, the normalized gage's length, and ε_{yk} denotes the strain in the k^{th} filament. The discrete averaging effects of a gage in the vicinity of a hole are function of the dimensions of the gage. It is advantageous to compare the size of the gage to the hole radius a. In the examples presented, it is assumed that the edge of the gage (or the first filament) is at distance $x_c=X_c/a$ from the edge of the hole and the vertical center of the gage is displaced from the lateral axis of the hole by $y_c=Y_c/a$, as shown in Fig 1. The width of the gage is $w=W/a$ and the filaments are evenly spaced across the width. The average strain now becomes a function of these variables and written as:

$$\varepsilon_{avg} = f(w, l_g, x_c, y_c, n) \qquad (7)$$

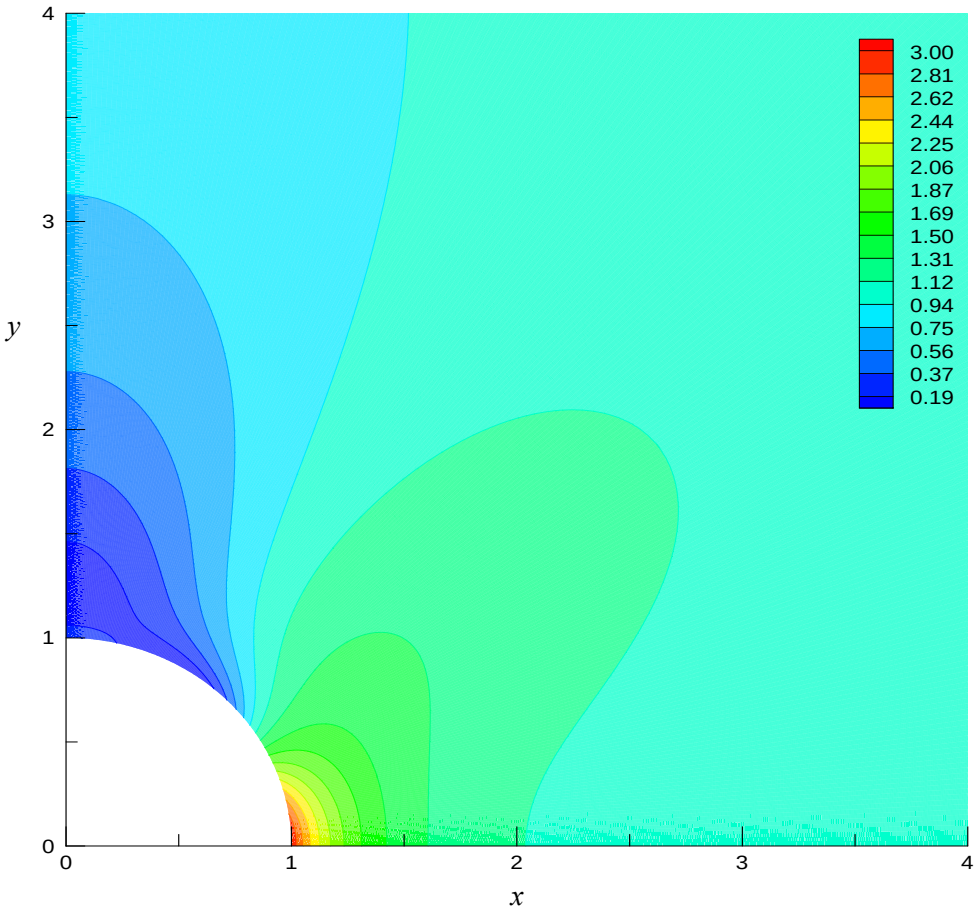

Figure 3. ε_y in the First Quadrant of the x-y Plane. σ_0/E=1 and ν=0.3.

RESULTS AND DISCUSSION

It is assumed that no shear lag occurs across the adhesive line, thus the strain felt by each gage filament is the same as the strain in the plate directly below it. The strain is averaged over each filament length. It is also assumed that the strain does not vary across an individual filament and the strains at the midline of the filaments are used in the averaging process. The filaments are evenly spaced across the width. Equations (6) and (7) provide a setting for evaluating the influences of each of the 5 parameters considered in this study. A few examples are presented to illustrate the magnitudes of error that are possible. The percent error e is defined with respect to the maximum normal strain that occurs at x=1 and y=0. In addition, the average strain $\bar{\varepsilon}_{avg}$ within the area A covered by the gage, which corresponds to the mathematical average strain for n=∞, is introduced for comparison:

$$\bar{\varepsilon}_{avg} = \lim_{n\to\infty} \frac{1}{nl_g} \sum_{k=1}^{n} \int_{l_g} \varepsilon_{yk}\, dy = \frac{1}{A} \int_A \varepsilon_y\, dA\,, \quad A = l_g w \qquad (8)$$

<u>Case 1</u>: In the first case the gage length is held constant while the gage width is varied with. Both X_c and Y_c are zero. Fig. 4 shows the variation of the averaging strain with the W/a for different number of filaments n. Additional filaments further away from the hole increases the error for a given width

gage. A single element at hole's edge gives an error of 7.24%. It is important to remember that these curves are for the same model, i.e. the same hole, material, and applied load, yet the strain is function of the gage width and the number of filaments. For W/a=0.5, the percent difference of the error between n=2 and n=10 is 16.6% while the percent difference of the error between n=2 and n=10 for W/a of 1.2 is 25.3%. One can conclude that the spacing between the filaments of a strain gage contributes to the error in measuring the strain. However, as an example for n=2, the percent difference of the error between W/a=0.5 and W/a=1.2 is 14.5%. Thus, the number of filaments is the dominant factor in the assessment of the error in strain gage measurements at the vicinity of stress concentration region. As a rule of thumb, the gage size should be very small as compared to the hole size. However, small strain gages tend to exhibit degraded performance in terms of the maximum allowable elongation, the stability under static strain, and the endurance when subjected to alternating cyclic strain [20].

Case 2: In this case, the gage width is kept constant and the gage length varied. The percentage error versus L_g/a for different number of filaments is shown in Fig. 5. It is clear that the average strain is a function of the gage length. However, for a given load the strain at the edge of the hole is constant. The difference in error between a single filament and two filaments is large for the same L_g/a ratios. It is clear that the multiple filaments tend to the same line for large L_g/a ratios. The results indicate that for L_g/a=0.5 the percent difference of the average strain between n=2 and n=10 is 16.7%. The percent difference in the average strain between L_g/a=0.5 and L_g/a=2 for n=2 is 35%. Therefore, both the gage length and the number of filaments should be considered in the assessment of the error of the average strain in the vicinity of stress concentration region. The user can select the smallest practicable gage

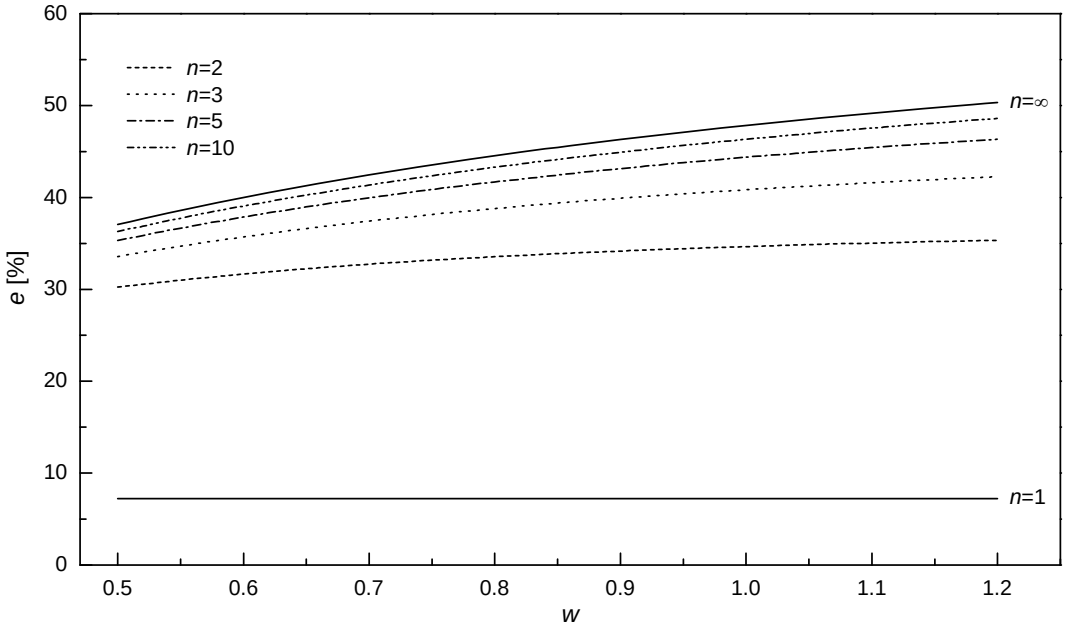

Figure 4. Effect of Gage's Size on Error Versus Width ($w=W/a$) for l_g=0.5 and $x_c=y_c$=0.

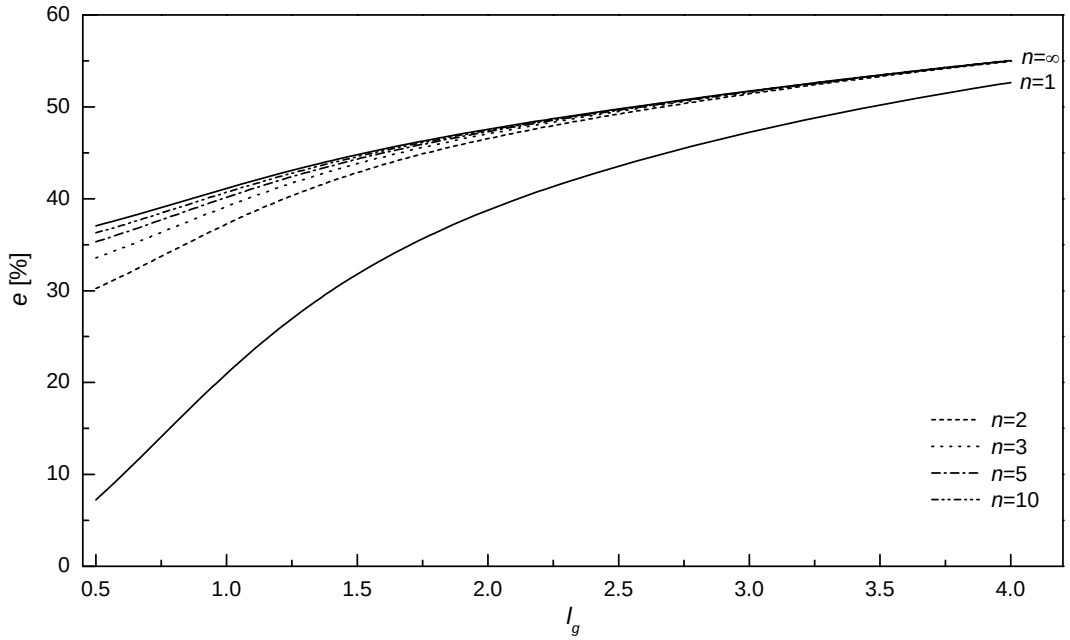

Figure 5. Effect of Gage's Size on Error Versus Length ($l_g=l_g/a$) for w=0.5 and $x_c=y_c$=0.

length, but has to be aware of the greatly increased error and uncertainty in the indicated strains due to the nature of the gage and instrumentations.

Case 3: In this case, both the gage length and width are held constant while the horizontal distance from the hole's edge to the first filament, X_c, varied. This is due to the facts that the matrix width of the strain gage is greater than the grid width and human-dependant error source. The metal-foil strain gage is the most frequently employed gage for both general-purpose stress analysis and transducer applications. The grids are very fragile and easy to distort, wrinkle, or tear. For this reason, foil gages are generally mounted on a thin epoxy carrier or paper or sandwiched (encapsulated) between two thin sheets of epoxy; this improves the temperature range, fatigue life, and chemical mechanical protection of the sensing grid. The dimensions of the matrix (sheets) are larger than that of the sensing grid. Hence, obtaining X_c=0 in engineering practice is very difficult. The results are plotted in Fig. 6. The percent difference of the error, for X_c=0, between n=2 and n=10 is 18.3%. But, for n=2, the difference of error between X_c/a=0 and X_c/a=0.5 is 47.5%. This clearly shows that the predominant factor in the error of the average strain is the lateral misdisplacement of the gage near the edge of the hole. The results also indicate that the number of filaments contributes significantly to the error of the strain measured at a stress concentration area.

Case 4: This case deals with the misplacement of the strain gage which is a typical human-dependant error. The distance between the hole's x axis and the gage horizontal center line is Y_c. Obtaining Y_c=0 in most practical situations is very difficult even for experienced operator with considerable skill and agility. Fig. 7 shows the strain averaging effect versus Y_c/a for $W=L_g$=0.5. The results show that the

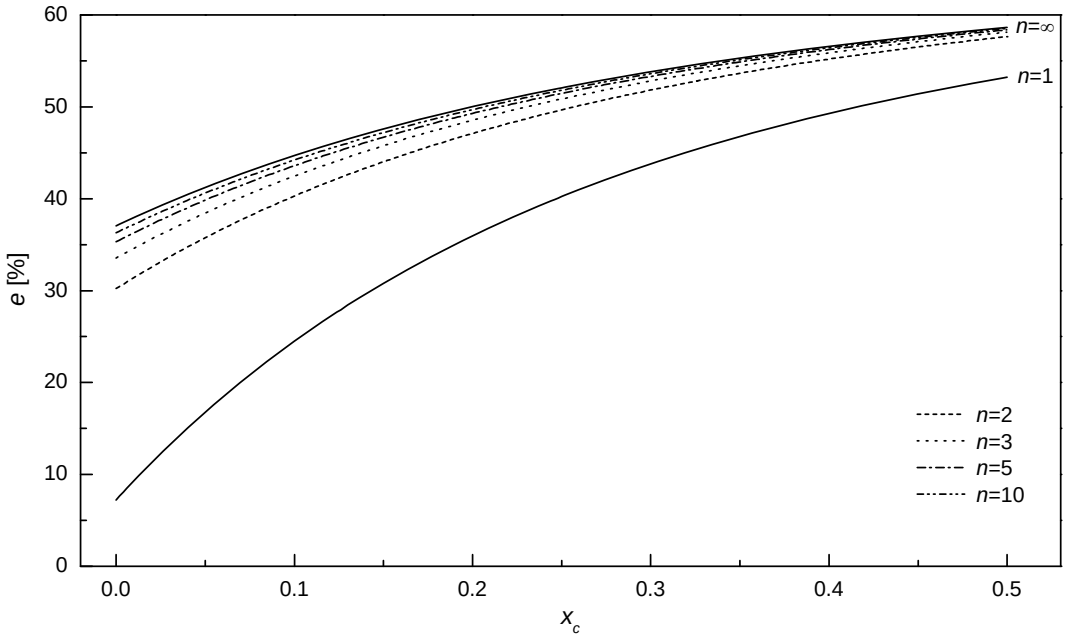

Figure 6. Effect of Gage's Alignment on Error Versus Lateral Alignment ($x_c=X_c/a$) for w=0.5 and l_g=0.5.

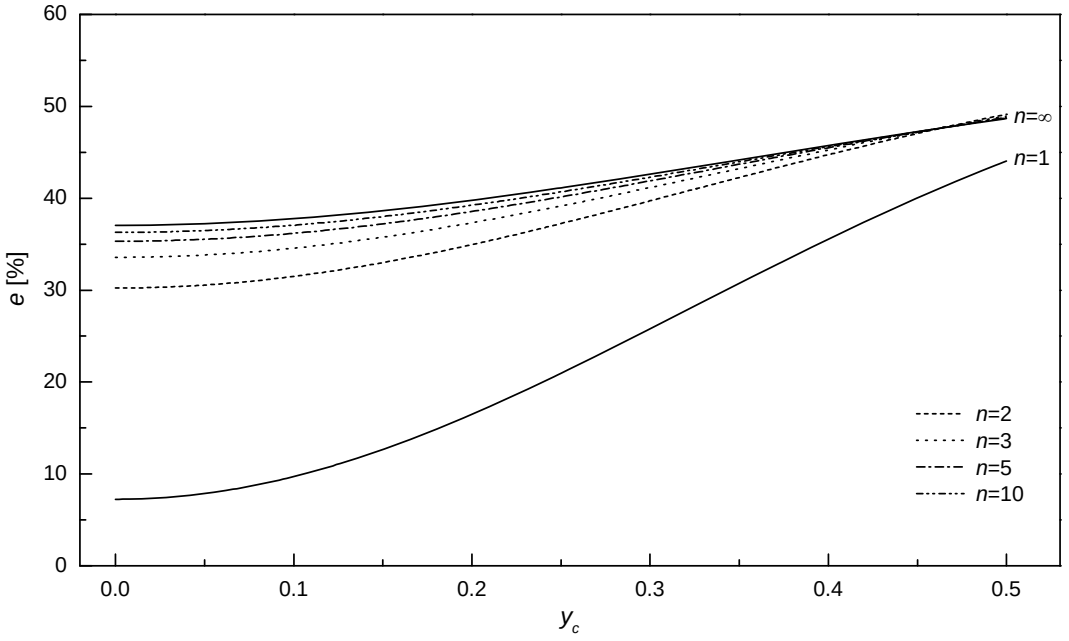

Figure 7. Effect of Gage's Alignment on Error Versus Vertical Alignment ($y_c=Y_c/a$) for w=0.5 and l_g=0.5.

number of filaments and the gage mispositioning contribute to the error of the average strain. For example, the percent difference of the average strain between n=2 and n=10 for perfect gage alignment is 16.5%. The difference of the average strain between properly aligned gage (n=2) and a gage displaced from the lateral axis of the hole by y_c=0.3 is 24% for n=2. From the results obtained, the error of measuring the strain at a the edge of a hole using strain gages can be clearly shown Figs. 4-7. Each line on the graphs represents the strain experienced by the gage for a given number of filaments.

As the number of filaments change, the strain also changes. Hence, the strain reading is a function of the number of filaments in the grid. The strain in the vicinity of a hole is constant at fixed applied load, but the strain gage results depend on the number of filaments. This shows that there is an error in the strain gage measurement and the number of filaments has a large influence on the average strain near a stress concentration area.

CONCLUSIONS

In this study, results of discrete averaging effects of a strain gage near a hole were presented. Four separate cases were investigated. Case 1 involved the effect of the gage width and case 2 examined the effect of the gage length. Cases 3 and 4 dealt with the mispositioning of the strain gage. In each case, the effects of the number of filaments upon the average strain were studied.

The existence of error can be seen by examining the variables of cases 1, 2, 3 and 4. When measuring the strain at the edge of a hole, the gage length and width present definite error. If these variables did not affect the strain average, the lines in Fig 4 would be horizontally linear. This is definitely not the case. Therefore, the magnitude of the strain gage reading error is dependent on the gage dimensions and position. The general trend of the strain gage reading (the average strain) is less than the actual strain as the distance from the hole increases. In addition, the average strain will decrease as the width of gage, length of the gage, or number of filaments in the grid increase. Therefore, the strain gage reading will underestimate the true strain at the edge of the hole. Thus, the number of gage filaments should be reduced in the hole-drilling method. The results can be used as a guide in correcting the measured strain at any circular hole.

Finally, the average strain over the gage filaments is not the same as the average strain over the gage grid area. This fact needs to be accounted for in determining stress concentrations using strain gages. The results show the error can be reduced significantly if an experimental stress analysis engineer selects a gage with a few filaments. There are at least 20 of filaments in most commercial strain gages. Therefore, a special purpose strain gages with few filaments should be manufactured and used for many practical applications.

REFERENCES

1. **Robinson, M., (2006)**, “Strain Gage Materials Processing, Metallurgy, and Manufacture”, Experimental Techniques 30, 42-46.
2. **Cappa, P., Del Prete, Z., and Marinozzi, F., (2001)**, “Long Term Stability of a Novel Strain Gage Conditioner Based on the Direct Resistance Method”, Experimental Techniques 25, 24-27.
3. **Ajovalasit, A., (2005)**, “Embedded Strain Gauges: Effect of the Stress Normal to the Grid”, Strain 41, 95-103.
4. **Ajovalasit, A., D’Acquisto, L., Fragapane, S., and Zuccarello, B., (2007)**, “Stiffness and

Reinforcement Effect on Electrical Resistance Strain Gauges", Strain 43, 299-305.

5. **Irwin, G. R., (1957)**, "Analysis of Stresses and Strains Near the end of a Crack Traversing a Plate", Applied Mechanics. 24.
6. **Dally, J. W. and Sanford, R. J., (1987)**, "Strain-Gage Methods for Measuring the Opening-Mode Stress-Intensity Factor, K_I", Experimental Mechanics 27, 381-388.
7. **Berger, J. R. and Dally, J. W., (1988)**, "An Overdeterministic Approach for Measuring K_I Using Strain Gages", Experimental Mechanics 28, 142-145.
8. **Berger, J. R. and Dally, J. W., (1988)**, "An Error Analysis for a Single Strain-Gage Determination of the Stress-Intensity Factor K_I", Experimental Techniques 12, 31-33.
9. **Marur, P. R. and Tippur, H. V., (1999)**, "A Strain Gage Method for Determination of Fracture Parameters in Bimaterial Systems", Engineering Fracture Mechanics 64, 87-104.
10. **Sarangi, H., Murthy, K. S. and Chakraborty, D., (2010)**, "Radial Locations of Strain Gages for Accurate Measurement of mode I Stress Intensity Factor", Materials & Design, in press.
11. **Zhang, S. Y., Prater, Jr., G., Shahhosseini, A. M., and Osborne, G. M., (2008),** "Experimental Validation of Structural Gage Sensitivity Indices for Vehicle Body Structure Optimization", Experimental Techniques 32, 51-54.
12. **Chen, J., Peng, Y., and Zhao, S., (2009)**, "Comparison Between Grating Rosette and Strain Gage Rosette in Hole-Drilling Combined Systems", Optics and Lasers in Engineering 47, 935-940.
13. **Barsanescu, P. and Carlescu, P., (2009)**, "Correction of Errors Introduced by Hole Eccentricity in Residual Stress Measurement by the Hole-Drilling Strain-Gage Method", Measurement 42, 474-477.
14. **Trench, P., Little, E. G., Tocher, D., O'Donnell, P., and Lawlor, V., (2009)**, "The Performance of Three-Dimensional Strain Rosettes Evaluated when Embedded into a Sphere", Strain 45, 149-159.
15. **Pople, J., (1984)**, "Error in Strain Measurement-the Human factor (or how much do I contribute?)", Experimental Techniques 8, 34-38.
16. **C. C. Perry, C. C., (1984)**, "The Resistance Strain Gage Revisited", Experimental Mechanics 24, 286-299.
17. **Stein, P. K., (1999)**, "Back to Basics", Experimental Techniques 23, 13-16.
18. **Philpot, T. A., (2008)**, Mechanics of Materials: An Integrated Learning System, John Wiley, USA, (2008).
19. **Dally, J. W. and. Riley, W. F., (1991)**, Experimental Stress Analysis, McGraw-Hill, New York, USA.
20. Strain Gage Selection, Criteria, Procedures, Recommendations. Tech. Note TN-505-1, Measurements Group, Inc., Raleigh, NC.